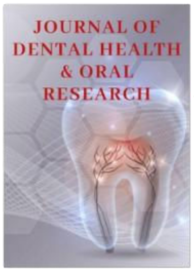

e-ISSN 3050-9432
Journal of Dental Health and Oral Research

ATHENAEUM SCIENTIFIC PUBLISHERS

Research Article

Check for updates

Mechanical Gradients in Adult Alveolar Cortical Bone under Orthodontic Tipping: A Finite Element Study (I)

Gilberto Salas[1*]

[1]Medical Stomatologist, Digital Orthodontist, Private practice in Alcoy, Spain

***Correspondence author:** Gilberto Salas, Medical Stomatologist, Digital Orthodontist, Private practice in Alcoy, Spain; E-mail: gilbertosalas42@gmail.com

Citation: Salas G. Mechanical Gradients in Adult Alveolar Cortical Bone under Orthodontic Tipping: A Finite Element Study (I). J Dental Health Oral Res. 2026;7(1):1-13.

https://doi.org/10.46889/JDHOR.2026.7120

Received Date: 26-01-2026

Accepted Date: 23-02-2026

Published Date: 02-03-2026

Abstract

Background: Orthodontic tooth movement in adults occurs within a mechanically constrained alveolar environment, where cortical bone remodeling capacity is limited and mechanical responses may be spatially heterogeneous.

Objectives: To characterize the spatial distribution of mechanical fields in adult alveolar cortical bone under coronal and radicular orthodontic tipping using finite element analysis.

Materials and Methods: A finite element model of a maxillary segment was constructed from cone-beam computed tomography data. Two orthodontic loading configurations were simulated: coronal tipping induced by aligner displacement and radicular tipping induced by a pure moment. Equivalent elastic strain, hydrostatic stress and principal stresses were analyzed to describe the spatial organization of the mechanical environment within the alveolar cortical bone.

Results: Both loading configurations generated heterogeneous and spatially organized mechanical fields rather than uniform stress or strain distributions. Coronal tipping produced localized strain and hydrostatic stress concentrations, predominantly in cervical cortical regions, whereas radicular tipping resulted in lower peak values and more evenly distributed mechanical gradients along the root length. In both scenarios, global strain magnitudes remained within low-to-moderate ranges consistent with an adult homeostatic context, while local gradients and stress transitions defined distinct mechanical domains.

Conclusion: Orthodontic tipping in adult alveolar cortical bone is characterized by structured mechanical fields governed by spatial gradients rather than by force magnitude alone. These findings are consistent with a gradient-based mechanical interpretation of Wolff's law in adult orthodontics, in which finite element analysis delineates zones of potential biological relevance without predicting direct remodeling outcomes.

Keywords: Orthodontic Biomechanics; Wolff's Law; Finite Element Analysis; Alveolar Cortical Bone; Mechanical Gradients; Adult Orthodontic

Introduction

Orthodontic Tooth Movement (OTM) is a biomechanical process arising from the interaction between applied orthodontic loads, the Periodontal Ligament (PDL) and the surrounding alveolar bone. Classical orthodontic theory describes this process through the pressure–tension paradigm, whereby bone resorption predominates on the compression side of the PDL and bone formation occurs on the tension side, enabling controlled dental displacement. This interpretation has traditionally been regarded as a clinical application of Wolff's law and as conceptually aligned with Enlow's architectural view of craniofacial adaptation [1,2,4]. However, this simplified paradigm assumes a relatively uniform and deterministic relationship between mechanical loading and bone remodeling. Contemporary mechanobiological evidence increasingly challenges this assumption, particularly in adult alveolar bone. Experimental, clinical and computational studies indicate that identical orthodontic force magnitudes may lead to markedly different biological outcomes depending on anatomical location, loading geometry and patient-specific biological context [3-15]. These findings indicate that orthodontic bone adaptation cannot be reliably inferred from force magnitude or local compression-tension states alone.

Beyond the periodontal ligament–centered interpretation, early biomechanical concepts questioned the assumption of a rigid alveolar housing. Structural theories proposed by Baumrind and later discussed by Grimm suggested that orthodontic forces may induce elastic bending of the alveolar bone itself, with the tooth acting as a lever within a deformable socket [5,6]. In this view, alveolar deformation contributes to the redistribution of mechanical stimuli within the bone rather than serving merely as a passive boundary to tooth displacement (Supplementary Fig. S1) [5,6].

Subsequent histological investigations provided indirect biological support for this structural intuition. Melsen and colleagues, studying orthodontic tooth movement in adult primates, observed patterns of bone apposition that could be interpreted as a response to bending-related tensile strain within the alveolar wall, rather than to localized periodontal compression alone [7]. These observations highlighted the constraining role of the alveolar cortical plate in adult patients and underscored the limited and non-uniform adaptive capacity of mature cortical bone during orthodontic treatment.

Over the past decade, advances in imaging, animal experimentation and computational biomechanics have substantially refined the understanding of orthodontic force transmission. High-resolution micro-computed tomography and histomorphometric studies have suggested that bone resorption and formation during OTM are spatially heterogeneous and frequently occur in adjacent regions rather than in strictly opposing compression and tension zones [8-10]. These findings are particularly pronounced in adult models, where orthodontic force–mediated bone remodeling is attenuated and bone turnover is reduced [16].

Finite element analyses further support this heterogeneity by revealing spatially non-uniform stress and strain fields within both the periodontal ligament and alveolar bone under orthodontic loading. Importantly, such analyses describe the mechanical environment generated by orthodontic forces without implying deterministic biological outcomes [13]. These results challenge mechanostat-inspired interpretations based on fixed mechanical thresholds, which assume predictable biological responses once a given strain magnitude is exceeded [1].

In this context, a gradient-based interpretation of orthodontic biomechanics offers a more coherent mechanical framework. Mechanical gradients describe the spatial variation of stress, strain and volumetric deformation within bone, rather than their absolute magnitudes. From a mechanobiological perspective, such gradients are particularly relevant because osteocyte networks are sensitive to spatial differences in deformation and associated fluid-induced shear, rather than to homogeneous static loading [14,15]. Importantly, the presence of mechanically plausible gradients does not imply guaranteed remodeling, especially in adult alveolar bone, where biological response remains conditional and patient-specific.

Therefore, the aim of this study was to characterize the spatial organization of strain and stress fields in adult alveolar cortical bone under coronal and radicular tipping using finite element analysis.

Materials and Methods

Finite Element Model

The finite element geometry was derived from a representative adult maxillary Cone Beam Computed Tomography (CBCT) dataset. Imaging parameters included a Field of View (FOV) of 8.19 × 8.19 × 8.19 cm and a voxel size of 0.16 mm. Reconstructed panoramic thickness was 5 mm with a slice interval of 1 mm. The dataset corresponded to a high-resolution dental CBCT volume. All image data were anonymized and used exclusively for modeling purposes. A representative maxillary segment including the tooth of interest and surrounding alveolar bone was isolated from the volumetric dataset. Semi-manual segmentation and trimming of the CBCT-derived geometry were performed using Meshmixer to obtain a geometrically consistent and numerically manageable region of interest suitable for finite element analysis. The segmentation and geometric processing workflow followed established finite element modeling approaches in orthodontic biomechanics [13].

The Periodontal Ligament (PDL) and alveolar bone layers were not directly segmented as independent anatomical entities from the CBCT. Instead, they were generated as offset structures based on clinically realistic thickness values, following established finite element modeling approaches in orthodontics [13]. The PDL was modeled with a uniform thickness of 0.2 mm, consistent with values commonly used in computational studies, while the alveolar cortical bone thickness was set to 1.7 mm [12]. This value was determined by direct inspection of cross-sectional CBCT slices using BlueSky software and lies within the reported range for adult alveolar cortical bone [13]. The resulting surface meshes were imported into ANSYS SpaceClaim, where mesh simplification and geometric refinement were performed to ensure numerical stability and compatibility with ANSYS Workbench. Boolean operations were applied to generate distinct solid bodies and to define contact interfaces between the tooth, periodontal ligament, alveolar bone and surrounding structures The modeling workflow and definition of contact interfaces followed standard procedures described in orthodontic finite element studies [13,16]. A horizontal attachment was designed and positioned on the tooth surface to enable controlled radicular tipping in the corresponding simulation scenario. The finalized solid geometry was then transferred to ANSYS Workbench for finite element analysis. Material properties were assigned in ANSYS Workbench to the tooth, periodontal ligament, cortical bone, alveolar bone, gingiva, attachment and aligner. All materials were modeled as homogeneous, isotropic and linearly elastic, as commonly assumed in orthodontic finite element analyses [13]. The finite element mesh consisted of tetrahedral elements. Contact interactions between solid bodies were defined as bonded, except for the contact between the aligner and the tooth surface, which was modeled as frictionless to allow relative sliding while transmitting normal contact forces, consistent with previous aligner-related finite element studies [16]. A fixed boundary condition was applied at the basal region of the maxillary sinus to prevent rigid body motion, following commonly adopted constraints in orthodontic finite element modeling [13]. Two loading configurations were simulated. In the coronal tipping configuration, tooth movement was induced by prescribing a lingual displacement of 0.25 mm at the aligner–tooth interface. No external force was directly applied; instead, contact pressure developed between the aligner and the tooth surface as a consequence of the imposed displacement. The resulting normal contact pressure reached values of approximately 0.14 MPa (compressive), leading to a reaction force of approximately 2.8 N transmitted through the aligner–tooth contact. This reaction force emerged naturally from the contact formulation and depended on the effective contact area rather than being imposed as an external load, in line with displacement-controlled orthodontic simulations [1]. The resulting force–moment system produced coronal tipping of approximately 2°. In the second scenario, radicular tipping was simulated by applying a pure moment of 30 N·mm, producing approximately 2° of vestibular root tipping with negligible net reaction force. This configuration was designed to isolate moment-dominated loading conditions, as commonly implemented in finite element studies of orthodontic mechanics [13]. The final finite element model consisted of approximately 65546 elements and 120421 nodes. The final finite element model is shown in Fig. 1.

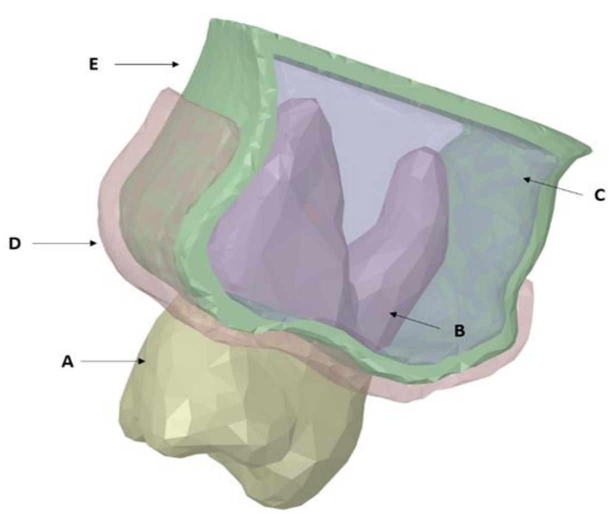

Figure 1: Finite element model geometry. Three-dimensional finite element model of the right maxillary first molar and surrounding supporting tissues. (A) Tooth (enamel–dentin complex). (B) Periodontal ligament (PDL) uniformly modeled around the root surface. (C) Alveolar bone compartment included in the model domain. (D) External soft-tissue envelope (gingiva/mucosa) retained for geometric continuity and excluded from mechanical analysis. (E) Alveolar cortical bone layer defined for stress and strain evaluation.

Mechanical Stimulus Definition (Gradient-Based Framework)

Equivalent Elastic Strain as A Scalar Field Descriptor

The following variables were defined to characterize the mechanical stimulus as a spatially organized field within adult alveolar bone. These descriptors were applied during post-processing and visualization and do not constitute biological thresholds, remodeling laws or predictors of tissue adaptation.

Mechanical deformation within the alveolar bone was characterized using equivalent elastic strain (ε_{eq}), defined as the von Mises strain derived from the principal strains, as commonly adopted in finite element analyses of bone mechanics [13,17].

$$\varepsilon_{eq} = \sqrt{\frac{1}{2}\left[(\varepsilon_1 - \varepsilon_2)^2 + (\varepsilon_2 - \varepsilon_3)^2 + (\varepsilon_3 - \varepsilon_1)^2\right]}$$

Equivalent elastic strain was used as a scalar descriptor of deformation intensity, allowing comparison of relative magnitudes within the alveolar cortical bone. In this study, ε_{eq} was not interpreted as a direct predictor of bone remodeling. Its role was to define a continuous mechanical field from which spatial gradients, contrasts and heterogeneities could be identified.

Particularly in adult alveolar bone, strain magnitude alone is insufficient to infer biological response [3,11]. Instead, the spatial organization of the strain field its gradients across cortical thickness, along the root axis and between vestibular and lingual plates was considered the primary mechanically meaningful feature [14,17]. The equivalent strain field distribution is illustrated in Fig. 2.

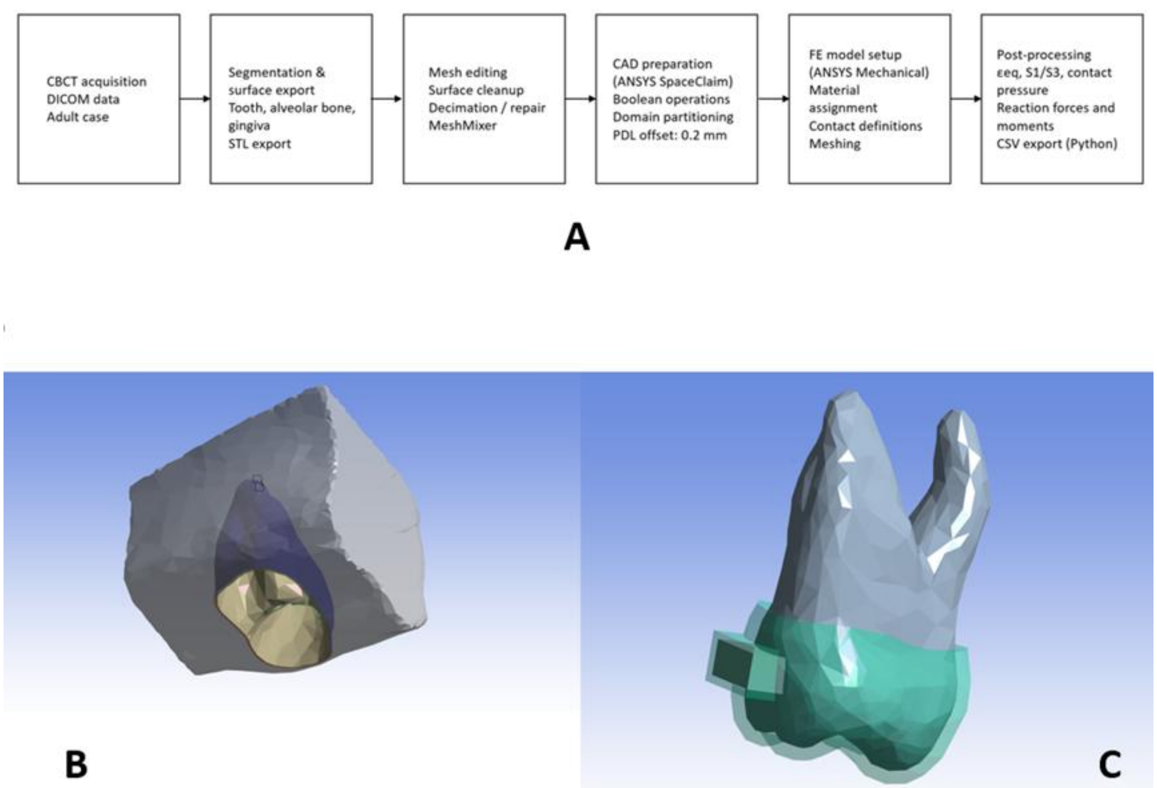

Figure 2: Finite element model construction. (A)Workflow from CBCT-based geometry reconstruction to finite element post-processing; (B) Bonded interfaces defined between the periodontal ligament and alveolar bone. (C) Orthodontic attachment and aligner geometry included to define mechanical interaction prior to load application.

Homeostatic Reference Strain as A Contextual Baseline

To contextualize the strain field within adult alveolar cortical bone, a reference strain level (ε_0) was introduced. This value represents a homeostatic mechanical context characteristic of adult cortical bone under sustained loading, rather than a biological activation threshold [1,17].

$$\varepsilon_0 = 300\ \mu\varepsilon$$

In adult bone, mechanical stimuli often operate close to equilibrium and deviations from this state do not necessarily result in active remodeling [1]. Accordingly, ε_0 does not represent a remodeling trigger or mechanostat threshold, but a contextual reference reflecting the mechanically constrained structural configuration characteristic of adult alveolar cortical bone [17].

A contrast measure Φ was defined as:

$$\Phi = \varepsilon_{eq} - \varepsilon_0$$

This relative formulation is consistent with gradient-based mechanical descriptions used in continuum bone modeling [1,17]. Φ serves as an indicator of spatial deviation from the adult mechanical baseline, identifying regions where strain intensity locally departs from the contextual reference state. It is introduced as a descriptive mechanical metric and does not imply a deterministic prediction of bone remodeling.

Hydrostatic Stress and Gradient-Based Interpretation

Hydrostatic stress (σh) was computed from the stress tensor as:

$$\sigma_h = \frac{1}{3}(\sigma_1 + \sigma_2 + \sigma_3)$$

following standard continuum mechanics formulations applied in bone mechanobiology [17].

Hydrostatic stress was used to distinguish compressive-dominated ($\sigma_h < 0$) and tensile-dominated ($\sigma_h > 0$) domains within the alveolar cortical bone [18]. Rather than focusing on absolute σ_h values, the analysis emphasized spatial variations and gradients of hydrostatic stress, particularly across cortical thickness and along the root surface. Recent finite element studies indicate that increased bone density and cortical stiffness may amplify hydrostatic stress under orthodontic loading without conferring adaptive advantage, highlighting that stress magnitude may reflect mechanical confinement rather than biological responsiveness [19]. These hydrostatic stress gradients are of specific mechanobiological relevance, as they reflect transitions between volumetric compression and dilation, which are known to influence interstitial fluid flow, vascular perfusion and osteocyte mechanosensing. In adult alveolar cortical bone, particularly within the thin buccal and lingual plates, such gradients may delineate regions of biological vulnerability or adaptation without implying a guaranteed remodeling response [14,15,17].

Characterization of Loading Nature Using Principal Stresses (S1-S3)

Because ε_eq and σ_h do not fully capture loading directionality, the nature of the mechanical stimulus was further characterized using principal stresses. Maximum (S1) and minimum (S3) principal stresses were extracted at the element level:

- S1 > 0 identifies tensile-dominated regions
- S3 < 0 identifies compressive-dominated regions

This separation allowed the mechanical environment to be described along two complementary dimensions:

1. Magnitude and spatial contrast (ε_eq, Φ)
2. Loading nature and directionality (S1, S3, σ_h)

By combining these descriptors, the analysis captures not only how intense the mechanical stimulus is, but also how it is organized spatially and mechanically, which is central to a gradient-based interpretation of Wolff's law [11,20].

Physiological Filtering of Numerical Singularities

Finite element simulations may exhibit localized stress or strain concentrations arising from geometric discontinuities or contact formulations that are not physiologically representative. To avoid overinterpretation of such numerical artifacts, a conservative upper physiological reference strain was introduced:

$$\varepsilon_{max} = 2000\ \mu\varepsilon$$

This value does not represent a remodeling or damage threshold. Instead, it serves as a conservative upper bound for physiological cortical bone strain ranges, consistent with mechanostat-based interpretations of bone mechanics [1].

Elements exceeding this value were excluded from mechanobiological interpretation but retained in the mechanical solution. This filtering step does not define a damage or remodeling threshold; rather, it ensures that gradient analysis reflects representative mechanical fields rather than isolated numerical peaks [1,11].

A percentile-based distribution analysis was performed as a descriptive post-processing check to verify that filtering did not alter the global spatial organization of the strain field.

Scope of the Mechanical Stimulus Framework

The variables defined above describe the spatial structure of the mechanical environment within adult alveolar bone under orthodontic loading. No remodeling law, temporal evolution or biological outcome is implied. By emphasizing strain gradients, hydrostatic stress transitions and tension–compression asymmetry, this framework provides a mechanically rigorous basis for identifying regions of potential biological relevance while explicitly acknowledging the constrained, non-deterministic nature of adult alveolar bone adaptation [3,17,20].

Mechanical stimuli were interpreted using a field-based framework in which hydrostatic and deviatoric components of deformation are treated as mechanically and energetically distinct quantities, consistent with continuum remodeling formulations proposed in non-orthodontic bone models (Fig. 3) [20].

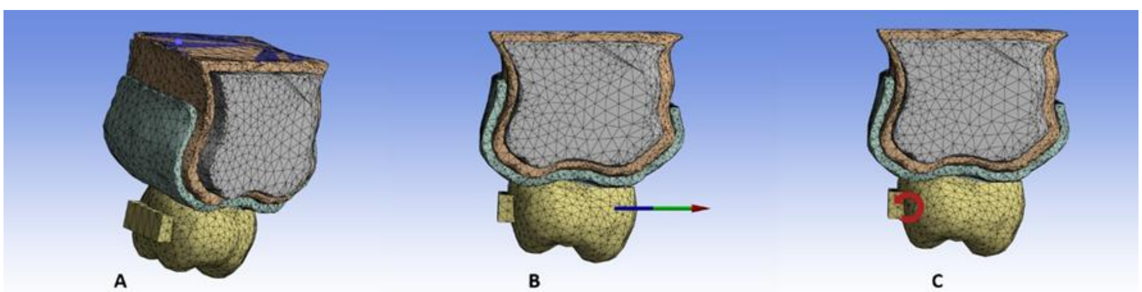

Figure 3: Boundary conditions and loading setup. (A) Fixed constraint applied to the basal surface of the bone segment; (B) Resultant contact force system generated by displacement-controlled aligner–tooth interaction; (C) Pure root-tipping moment (30 N·mm) applied to simulate radicular tipping.

Results

Two distinct orthodontic loading scenarios were simulated: coronal tipping induced by an imposed coronal displacement and radicular tipping induced by an applied pure moment. In the coronal tipping configuration, a horizontal displacement of 0.25 mm was imposed at the coronal region of the tooth. Despite this prescribed unidirectional displacement, the resulting total deformation reached 0.38 mm, reflecting the contribution of rotational components and secondary displacements arising from tooth–aligner contact and geometric constraints. This confirms that the imposed boundary condition generated a combined translational–rotational movement rather than a rigid body translation. The prescribed displacement generated a compressive contact pressure of approximately 0.14 MPa at the aligner–tooth interface, resulting in a reaction force of approximately 2.8 N. This force arose from the contact interaction and was not imposed directly, confirming that the simulated loading conditions reflect aligner-mediated mechanics rather than force-controlled orthodontic systems. In the radicular tipping configuration, a pure moment of 30 N·mm was applied. The resulting displacement field showed a rotational pattern characterized by limited coronal translation and a predominant angular response, consistent with a root-controlled tipping mechanism. These results confirm that the two loading configurations produced mechanically distinct movement patterns (Fig. 4) [14].

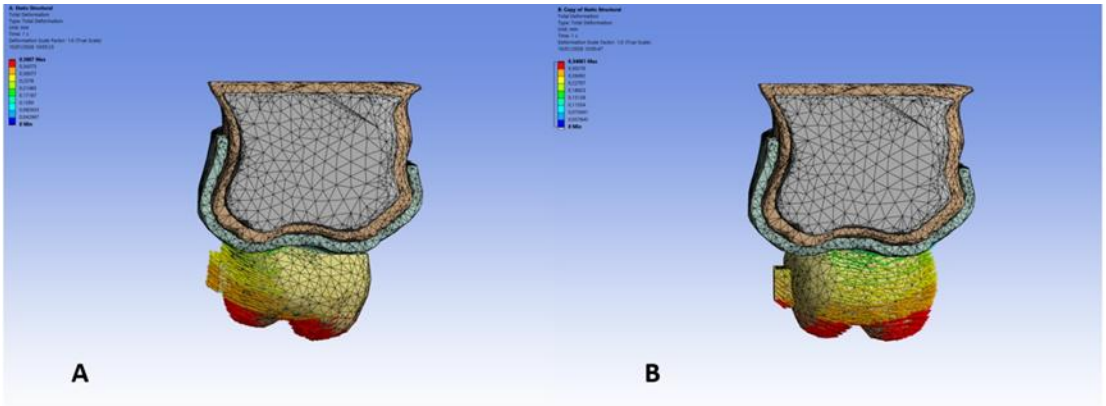

Figure 4: Kinematic outcome of the simulated orthodontic tipping scenarios. A) Displacement field generated by coronal tipping induced by an imposed horizontal displacement at the crown, showing a combined translational–rotational response; (B) Displacement field generated by radicular tipping induced by a pure moment of 30 N·mm, showing predominant angular displacement with minimal coronal translation.

Reaction forces and moments were extracted at the constrained boundary conditions to characterize the global force system generated by each simulation. In the radicular tipping scenario, the resultant reaction force was approximately zero, indicating the absence of net translational loading and confirming that the applied load acted as a pure couple. In contrast, the reaction moment balanced the applied moment, with a magnitude close to 30 N·mm, as expected from static equilibrium.

In the coronal tipping scenario, 2.4 N force was observed due to the imposed displacement and contact interactions, reflecting a combined force–moment system. These results validate the mechanical consistency of both simulations and confirm that the intended loading conditions were correctly implemented. Contact pressure at the aligner–tooth interface was spatially non-uniform in both loading configurations. Peak pressures were localized around the attachment edges and decreased rapidly with distance from the contact region. Overall, contact pressure magnitudes remained low and broadly distributed, reflecting the compliant nature of the aligner material and the displacement-controlled loading strategy, in agreement with previous finite element analyses of aligner biomechanics [20].

In the coronal tipping simulation, contact pressure was distributed over a contact area of approximately 37.0 mm², with peak pressures on the order of 0.14 MPa. The pressure distribution was spatially coherent with the imposed coronal displacement and exhibited no localized high-pressure peaks. The radicular tipping simulation showed a distinct contact pattern consistent with moment-driven loading, characterized by opposing regions of contact pressure corresponding to the generated couple. Overall, contact pressures remained low in both configurations, consistent with the distributed and compliant nature of aligner-mediated force application.

Both coronal and radicular tipping configurations generated heterogeneous mechanical fields within the alveolar cortical bone. Rather than exhibiting uniform stress or strain distributions, the simulations revealed spatially organized patterns of deformation intensity that varied across cortical thickness and along the root surface, a characteristic feature of orthodontic finite element models [11,17].

Equivalent elastic strain values predominantly remained within low-to-moderate ranges relative to adult cortical bone, with no extensive regions exceeding the contextual baseline reference strain. This finding is consistent with experimental and imaging studies reporting reduced remodeling activity and constrained adaptive capacity in adult alveolar bone [16,13].

Analysis of the strain field revealed consistent cortical gradients, with higher deformation intensities localized near the alveolar crest and progressive attenuation toward the basal cortical regions. These gradients were present in both loading configurations, although their spatial orientation and magnitude differed between coronal and radicular tipping, supporting a gradient-based interpretation of orthodontic loading [17,18].
Hydrostatic stress analysis further refined the characterization of the mechanical environment. Regions of compressive-

dominated volumetric stress were spatially confined and closely associated with areas of increased geometric constraint. Elevated hydrostatic stress emerged preferentially in dense cortical regions, reflecting mechanical confinement rather than applied force magnitude, a pattern previously linked to non-adaptive biological responses in orthodontic loading [21,22]. Elements exceeding a conservative upper physiological reference strain were sparse and spatially isolated. Exclusion of these elements from gradient analysis did not alter the overall spatial organization of the mechanical field, supporting the interpretation that the observed patterns reflect representative mechanical behavior rather than numerical singularities [1]. Taken together, these results suggest that orthodontic tipping generates structured mechanical fields characterized by spatial gradients, stress transitions and directional asymmetry, rather than uniform deformation states, reinforcing a non-deterministic mechanical description of orthodontic loading (Fig. 5) [17,3].

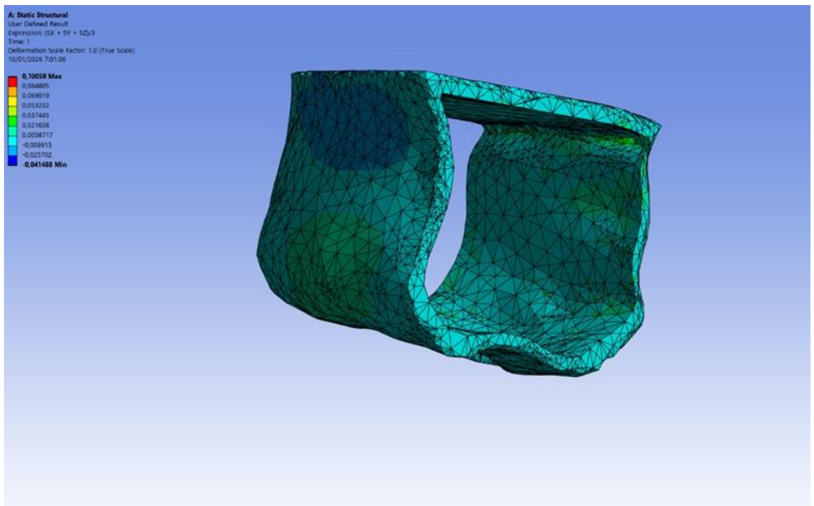

Figure 5: Hydrostatic stress distribution and volumetric stress transitions in adult alveolar cortical bone. Hydrostatic stress (σ_h) distribution within the alveolar cortical plate under orthodontic loading, illustrating spatial transitions between compressive and tensile volumetric stress domains across cortical thickness and along the root axis. Results correspond to the coronal tipping configuration.

To characterize the nature of the mechanical stimulus, maximum and minimum principal stresses were analyzed. Regions dominated by compressive loading (S3 < 0) were primarily located at the cortical alveolar plate toward which the tooth rotated, whereas tensile-dominated regions (S1 > 0) were observed on the opposing side. This spatial separation of compressive and tensile domains was consistent across both tipping configurations, although their extent and localization differed between coronal and radicular tipping. This distribution is consistent with classical biomechanical interpretations of alveolar deformation under orthodontic loading, in which the alveolar bone behaves as a deformable structure rather than a rigid housing [5,6]. The radicular tipping scenario produced a more balanced distribution of compressive and tensile regions along the root length, whereas coronal tipping resulted in more localized stress concentrations near the cervical cortical bone (Fig. 6).

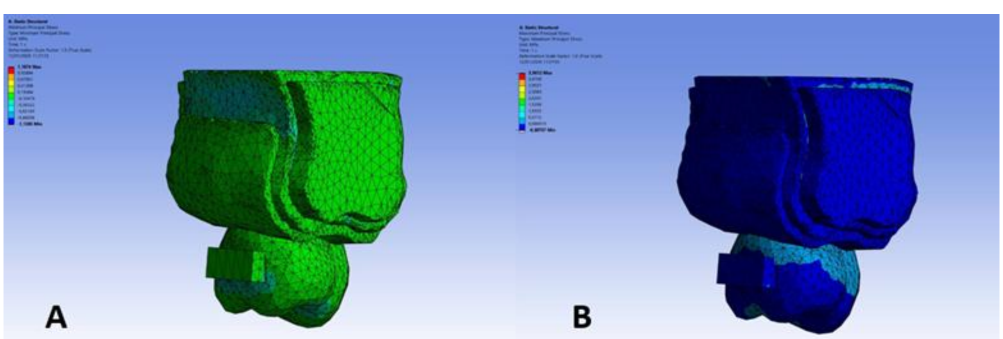

Figure 6: Principal stress domains in the alveolar cortical bone under orthodontic loading. (A) Minimum principal stress (S3) distribution identifying compressive-dominated regions in the alveolar cortical bone; (B) Maximum principal stress (S1) distribution identifying tensile-dominated regions on the opposing cortical surface.

Taken together, the results suggest that coronal and radicular tipping generate distinct global force systems, contact mechanics and alveolar bone stimulus distributions. While both configurations operate within a low-force, low-pressure regime compatible with aligner mechanics, their strain and stress patterns differ in spatial organization and relative dominance of compressive versus tensile loading. These differences provide a mechanical basis for interpreting distinct biological responses under adult orthodontic conditions, without assuming proportional or guaranteed bone adaptation. These findings underscore those orthodontic biomechanics in adult bone are governed by spatial organization of the mechanical field rather than by force magnitude alone [3].

Discussion

The present finite element simulations provide a mechanical interpretation of coronal and radicular tipping under aligner-mediated orthodontic loading in an adult scenario. Rather than assuming a direct proportional relationship between applied loads and bone adaptation, the results describe the distribution and nature of the mechanical stimulus acting on the alveolar bone, in line with a constrained and age-dependent interpretation of Wolff's law [1,3,15].

Both tipping configurations generated mechanically coherent movement patterns, as confirmed by the kinematic outcomes and global reaction forces and moments. Coronal tipping induced by an imposed displacement resulted in a combined force–moment system, whereas radicular tipping induced by a pure moment produced negligible net reaction forces and a balanced moment response. This distinction is fundamental, as it suggests that similar clinical tooth movements may arise from fundamentally different mechanical loading regimes at the tooth–bone interface [14,20].

The present results indicate that, in the adult alveolar bone context, the mechanical environment generated by orthodontic tipping is best understood in terms of spatial organization and gradients, rather than absolute stimulus magnitude [3,17,18].

Equivalent elastic strain values remained predominantly within low-to-moderate ranges across both loading configurations. However, in the framework adopted in this study, this observation is not interpreted as evidence of insufficient stimulation for bone adaptation. Instead, it reflects the fact that adult alveolar cortical bone operates close to a mechanical homeostatic state, in which global strain magnitudes are tightly regulated and large deviations are uncommon under clinically realistic orthodontic loading [1,15,16].

Within this near-homeostatic context, the mechanically relevant information is conveyed by local contrasts and gradients within the strain and stress fields, rather than by peak values. The finite element results suggested that deviations from the adult contextual baseline were spatially confined and organized into coherent patterns, particularly across cortical thickness, along the root axis and between vestibular and lingual cortical plates [17,18]. From a mechanobiological perspective, this organization is consistent with current evidence indicating that adult bone adaptation is not driven by the magnitude of sustained mechanical loading alone, but by the heterogeneity and directional structure of the mechanical field [3,17]. In adult alveolar bone, sustained loading near equilibrium may preserve structural stability, while localized gradients may delineate zones of potential biological sensitivity or vulnerability, depending on the local biological context [16].

Importantly, the absence of widespread high-magnitude strain does not imply mechanical irrelevance. Rather, it underscores the constrained adaptive capacity of adult alveolar bone, where mechanical loading primarily modulates existing structural equilibrium rather than inducing robust anabolic remodeling [1,15,16]. Accordingly, the present findings support a shift away from interpreting adult orthodontic biomechanics through the lens of strain sufficiency or deficiency. Instead, they favor a gradient-based view in which mechanical loading defines a spatial map of constrained possibilities, within which biological response remains conditional, localized and highly dependent on patient-specific factors [3,17,18].

The analysis of principal stresses revealed a clear spatial organization of compressive and tensile domains within the alveolar cortical bone. Regions dominated by compressive loading ($S3 < 0$) were consistently located on the cortical plate toward which the tooth rotated, whereas tensile-dominated regions ($S1 > 0$) appeared on the opposing side. This arrangement reflects the asymmetric transfer of orthodontic loads across the alveolar socket and is consistent with classical mechanical descriptions of tooth movement [5,6]. Importantly, in the present framework, compression and tension are not interpreted as binary biological triggers leading directly to bone resorption or apposition. Instead, they are considered mechanical descriptors of loading nature, whose biological relevance depends on their spatial distribution, gradients and interaction with local tissue context [3,7]. In the adult alveolar bone scenario examined here, compressive and tensile regions were not uniformly distributed nor sharply delimited. Rather, they formed continuous spatial transitions, particularly across cortical thickness and along the root surface. Such transitions are mechanically significant because they define gradients in volumetric deformation and stress state [17,18,22]. Accordingly, the presence of compressive- or tensile-dominated regions should be understood as defining mechanically distinct environments, not guaranteed biological outcomes. In adult patients, age-related reductions in bone plasticity and adaptive capacity further constrain the translation of these mechanical cues into effective remodeling (Fig.7) [15,16].

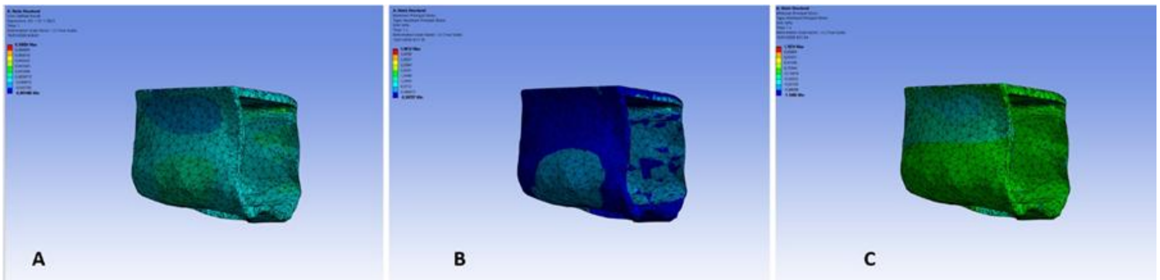

Figure 7: Integrated spatial organization of mechanical gradients in adult alveolar cortical bone. (A) Compressive-dominated regions derived from minimum principal stress (S3); (B) Tensile-dominated regions derived from maximum principal stress (S1); (C) Integrated schematic illustrating the spatial organization of mechanical gradients across the alveolar cortical bone.

The comparison between coronal and radicular tipping highlights that distinct mechanical strategies lead to different alveolar bone stimulus distributions, even when the resulting tooth movement appears clinically similar. Coronal tipping tended to concentrate mechanical effects near the cervical cortical bone, whereas radicular tipping produced a more distributed pattern along the root length.

From a biomechanical standpoint, this distinction may be particularly relevant in adult patients, where cervical cortical bone is often thin and vulnerable to maladaptive responses [13,16,21]. The results suggest that root-controlled tipping, achieved through moment-dominant loading, may offer a more spatially balanced mechanical environment, potentially reducing localized cortical overload [14,20]. The present findings support a conditional and spatially constrained interpretation of Wolff's law in adult orthodontics. This interpretation is strictly mechanical in nature and does not propose a biological remodeling law or deterministic adaptive mechanism. Mechanical loading remains a necessary driver of alveolar bone response; however, its biological effects cannot be inferred from stimulus magnitude alone, nor assumed to operate uniformly across the loaded structure [1,3].

In adult alveolar bone, mechanical adaptation appears to occur within a restricted homeostatic regime, where sustained orthodontic forces primarily redistribute mechanical fields rather than induce widespread anabolic remodeling [1,15,16]. Within this regime, the spatial organization of mechanical gradients including strain heterogeneity, hydrostatic stress transitions and tension–compression asymmetry defines regions of potential biological relevance without prescribing a specific remodeling outcome [17,18,22]. Rather than conceptualizing bone response in terms of fixed adaptive windows or threshold-driven transitions, the present framework emphasizes gradient-limited adaptation [17]. Mechanical gradients delineate zones of differential mechanical context, within which biological response remains conditional, localized and modulated by patient-specific factors such as age, vascularity and inflammatory status [15,16]. This reinterpretation aligns Wolff's original principle of functional adaptation with contemporary mechanobiological evidence, while avoiding deterministic predictions [1,3]. From a mechanobiological perspective, the gradient-based mechanical environments identified in this study may be interpreted as permissive contexts for organized bone adaptation, (Supplementary Fig. S2). This framework does not propose a new biological law, but a mechanical interpretation consistent with existing mechanobiological evidence. While the present study does not attempt to model biological remodeling, recent advances in mechanobiology provide insight into how mechanically computed stimuli may be sensed at the cellular level. Mechanosensitive ion channels such as PIEZO1 have been identified as key mediators of cellular responses to mechanical loading in bone and periodontal tissues, providing a plausible mechanistic link between spatial strain and stress distributions and downstream biological signaling [19]. Importantly, the presence of such mechanotransduction pathways does not imply a deterministic remodeling outcome, particularly in adult alveolar bone [3,15].

A key methodological contribution of this work lies in the explicit separation between mechanical computation and biological interpretation. Finite element analysis was used solely to compute mechanical fields, while the definition of remodeling-relevant variables was performed through post-processing, in line with recommendations to avoid embedding speculative biological laws within numerical solvers [11,17]. Clinically, the results underscore the importance of understanding not only the magnitude of orthodontic forces but also their mechanical nature and spatial distribution. In adult orthodontics, strategies that minimize localized compressive overload while maintaining controlled movement may be preferable to aggressive force application [14,21].

Limitations

This study is subject to several limitations. The finite element simulations were static and did not include temporal evolution, biological feedback or remodeling algorithms. Material properties were assumed to be homogeneous, isotropic and linearly elastic. No histological or clinical validation was performed. Accordingly, the results should be interpreted as a description of mechanical field organization rather than as predictors of biological response or clinical outcome.

The present study establishes a mechanically rigorous description of the spatial organization of stress and strain gradients in adult alveolar cortical bone under orthodontic tipping. By deliberately separating mechanical field computation from biological interpretation, this work defines the boundary conditions within which any adaptive response may occur, without assuming remodeling as an inevitable outcome. Building on this mechanical foundation, a subsequent study (Part II) will extend the present framework by introducing a time-dependent, mechanobiological formulation aimed at exploring how spatially organized mechanical gradients may interact with cellular mechanotransduction pathways and bone turnover dynamics under adult orthodontic conditions.

Conclusion

Orthodontic tipping in adult alveolar cortical bone generates heterogeneous and spatially organized mechanical fields rather than uniform stress or strain distributions. Finite element analysis shows that coronal and radicular tipping strategies produce distinct patterns of strain, hydrostatic stress and principal stress organization, despite similar macroscopic tooth movements. In the adult context, global strain magnitudes remain close to a homeostatic range, while local gradients and stress transitions define mechanically distinct domains. These findings support a non-deterministic, gradient-based interpretation of Wolff's law in adult orthodontics, in which mechanical loading delineates zones of potential biological relevance rather than guaranteeing remodeling. This framework emphasizes spatial organization over force magnitude when interpreting orthodontic biomechanics in mature alveolar bone.

Conflict of Interest

The authors declared no potential conflicts of interest with respect to the research, authorship and/or publication of this article.

Funding Statement

This research did not receive any specific grant from funding agencies in the public, commercial or non-profit sectors.

Acknowledgement

None.

Data Availability Statement

Not applicable.

Ethical Statement

The project did not meet the definition of human subject research under the purview of the IRB according to federal regulations and therefore, was exempt.

Informed Consent Statement

Informed consent was taken for this study.

Authors' Contributions

The author(s) conceived the editorial concept, reviewed relevant literature, drafted the manuscript and approved the final version for publication.

References

1. Frost HM. A 2003 update of bone physiology and Wolff's law for clinicians. Angle Orthodontist. 2004;74(1):3-15.
2. Isola G, Matarese M, Briguglio F, Grassia V, Picciolo G, Fiorillo L. Mechanobiology of tooth movement during orthodontic treatment: a literature review. Minerva Stomatologica. 2016;65(6):299-327.
3. Li Y, Jacox LA, Little SH, Ko CC. Biomechanical and biological responses of periodontium in orthodontic tooth movement: Update in a new decade. International Journal of Oral Science. 2021;13(1):20.
4. Enlow DH, Hans MG. Essentials of facial growth. Philadelphia: Saunders. 1996.
5. Baumrind S. A reconsideration of the propriety of the pressure-tension hypothesis. American Journal of Orthodontics. 1969;55(1):12-22.
6. Grimm FM. Bone bending, a feature of orthodontic tooth movement. American Journal of Orthodontics. 1972;62(4):384-93.
7. Melsen B. Biological reaction of alveolar bone to orthodontic tooth movement. Angle Orthodontist. 1999;69(2):151-8.
8. Zong C, Liu Y, Wang J, Zhang X, Li Y, Chen Z, et al. Dynamic changes in tooth displacement and bone morphometry induced by orthodontic force: A longitudinal micro-CT study. Scientific Reports. 2022;12:13672.
9. Trelenberg-Stoll V, Faber J, Bumann A, Jäger A, Müller M, Wehrbein H, et al. Standardized assessment of bone micromorphometry around teeth following orthodontic tooth movement: A micro-CT split-mouth study in mice. Journal of Orofacial Orthopedics. 2022;83(5):403-11.
10. Rizk M, Ghoneima A, Del Fabbro M, Pandis N, Fudalej P, Park J, et al. Periodontal ligament and alveolar bone remodeling during long orthodontic tooth movement: a 3D micro-CT analysis in mice. Scientific Reports. 2023;13:19919.
11. Ren Y, Maltha JC, Kuijpers-Jagtman AM. Age-dependent responses of alveolar bone to orthodontic force in rats. American Journal of Orthodontics and Dentofacial Orthopedics. 2019;156(5):620-30.
12. Zhang R, Zhang L, Wang Z, Wu Z. Influence of periodontal ligament heights on sequential and simultaneous maxillary molar distalization using clear aligners. Pakistan Journal of Medical Sciences. 2025;41(8):2279-84.
13. Cattaneo PM, Dalstra M, Melsen B. The finite element method: a tool to study orthodontic tooth movement. Journal of Dental Research. 2005;84(5):428-33.
14. Gross TS, Edwards JL, McLeod KJ, Rubin CT. Strain gradients correlate with sites of periosteal bone formation. Journal of Bone and Mineral Research. 1997;12(10):1603-13.
15. Jiang Y, Liu X, Chen L, Wang Y, Li Z, Zhang H, et al. Mechanosensitive Piezo1 in periodontal ligament cells promotes alveolar bone remodeling during orthodontic tooth movement. Frontiers in Physiology. 2021;12:767136.
16. Gómez JP, Peña FM, Martínez V, Giraldo DC, Cardona CI. Initial force systems during bodily tooth movement with plastic aligners and composite attachments: a three-dimensional finite element analysis. Angle Orthodontist. 2015;85(3):454-60.
17. Branecka N, Yildizdag ME, Ciallella A, Giorgio I. Bone remodeling process based on hydrostatic and deviatoric strain mechano-sensing. Biomimetics. 2022;7(2):59.
18. Wang J, Huang Y, Chen F, Li W. The age-related effects on orthodontic tooth movement and the surrounding periodontal environment. Frontiers in Physiology. 2024;15:1460168.
19. Kuc AE, Sybilski K, Stankiewicz M, Kotuła J, Kuc N, Hajduk G, et al. The influence of bone density on stresses in the periodontal ligament during orthodontic movement: finite element study on innovative model. Materials. 2025;18(4):776.
20. Tiwari AK, Goyal A, Prasad J. Modeling cortical bone adaptation using strain gradients. Proceedings of the Institution of Mechanical Engineers Part H. 2021;235(5):09544119211000228.
21. Yaseen TA, Younis H, Aghayants S, Yin M, Cheng B. Impact of vertical facial type on alveolar bone thickness and tooth morphology: A retrospective CBCT-based clinical study. Journal of Stomatology Oral and Maxillofacial Surgery. 2024;125(6):102128.
22. Wang X, Xue J, Wang X, Fan M. Biomechanical effects of orthodontic tooth movement on edentulous alveolar bone: A finite element analysis. Frontiers in Bioengineering and Biotechnology. 2025;13:1625027.

Supplementary Information

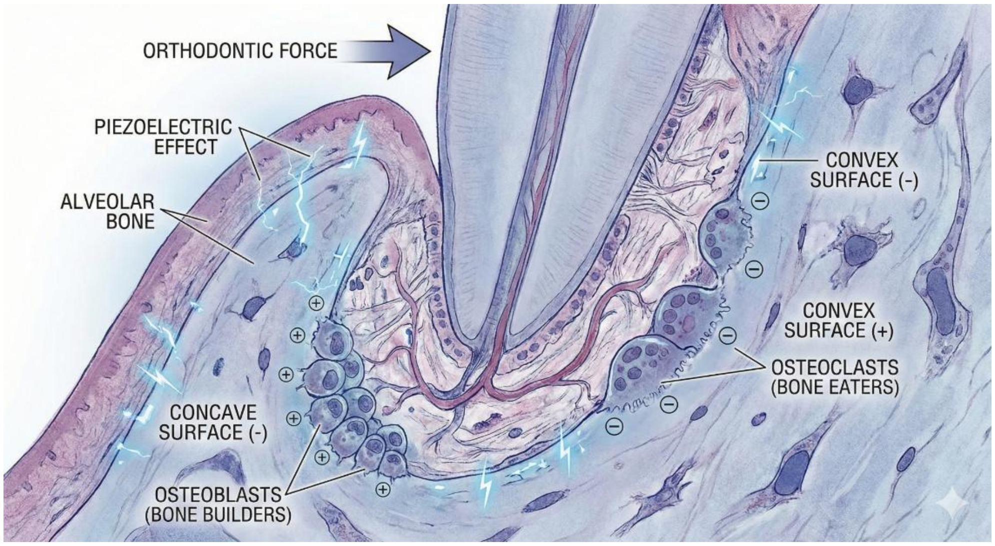

Supplementary Figure S1: Conceptual representation of alveolar bone deformation under orthodontic loading, contrasting the traditional rigid alveolar housing assumption with a deformable bone bending model. The schematic highlights the emergence of spatially heterogeneous mechanical fields within the alveolar complex and provides a conceptual basis for the gradient-based interpretation adopted in this study.

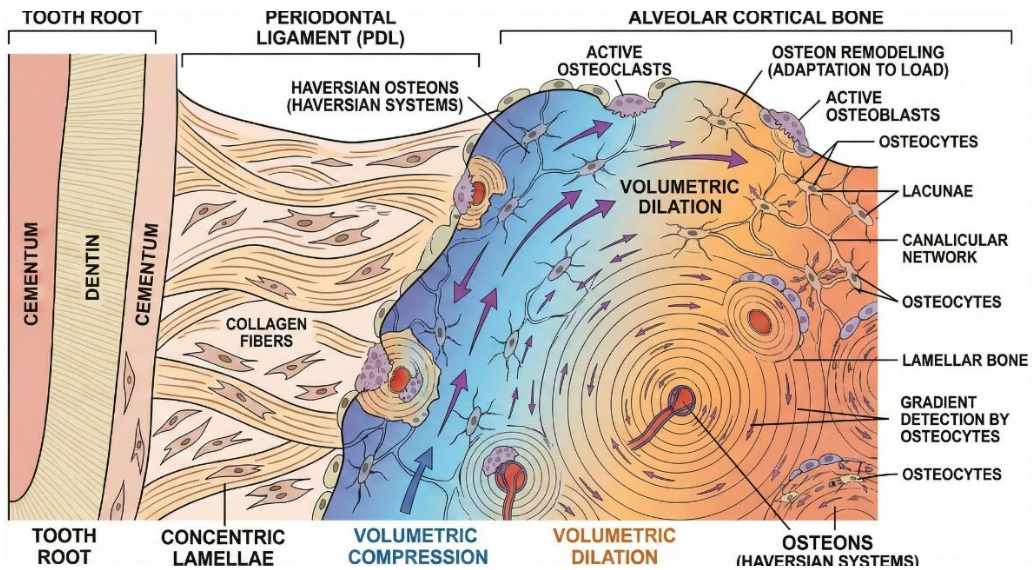

Supplementary Figure S2: Schematic representation of the gradient-based mechanical framework, integrating equivalent elastic strain (ε_{eq}), hydrostatic stress (σ_h) and principal stress asymmetry (S1–S3) within an adult cortical bone homeostatic context. The diagram illustrates how spatial gradients, rather than absolute magnitudes, define mechanically distinct domains without implying deterministic biological remodeling.